JOURNAL OF CATALYSIS 29, 49–59 (1973)

Catalytic Activity of Organic Semiconductors. Hydrogen Conversion on Triphenylene–Alkali Metal Ion Radical Salts

KEISAKU KIMURA AND HIROO INOKUCHI

The Institute for Solid State Physics, The University of Tokyo, Roppongi, Tokyo

Received June 20, 1972

An extensive study was made of the kinetics and the mechanism of the ortho–parahydrogen conversion, the deuterium exchange reaction, and the hydrogen–deuterium equilibration over solid triphenylene–alkali metal ion radical salts (K-, Rb-, and Cs- salts). Two species, mono- and dinegative anion salts, were stoichiometrically prepared. Two different reaction paths, one through the chemisorption process and the other via the exchange process, were observed. With simultaneous measurements of the rate of hydrogen adsorption and also of the time course of ortho–parahydrogen conversion on the salt catalysts, a novel kinetic analysis, based on the two processes, was presented. In comparing these processes, the chemisorption process was found to be predominant in every reaction over the complexes in question. Further, it was observed that the catalytic activity depends strongly on the valency of anions and on the sort of alkali metal; the rate constant of the dianion salt was much larger than that of the monoanion salt, and the activity increased in the order of K, Rb, and Cs.

INTRODUCTION

Since the catalytic activities of aromatic–alkali metal ion salts for the ortho–parahydrogen conversion and the hydrogen–deuterium exchange reaction were found (*1*, *2*), a number of papers concerning the catalytic behavior have been published (*3–12*). However, the catalytic mechanisms and the factors governing the activities have not yet been clarified sufficiently. There are several hypotheses as to the mechanism, such as that the activities depend on the delocalization energy of aromatics and/or that the electron affinity of aromatics has a close relation to the activities. These proposals, however, have been based on experiments in which the rate constant was calculated from the tangent of the initial slope of the time course of the reaction, and no detailed analysis of the whole reaction has been carried out. Further, the role of alkali metal in the reaction has hardly been clarified (*10*).

Recently, two proposals concerning these reaction mechanisms have been made. Tanaka *et al.* (*11*) reported the occurrence of the hydrogen–deuterium exchange reaction on the anthracene–Na complex via monohydroanthracene. On the other hand, Tsuda (*10*) proposed two paths for the hydrogen–deuterium exchange reaction on the benzonitrile–alkali metal complex; one is the "chemisorption mechanism" and the other the "exchange mechanism." Previously, Wakayama and Inokuchi (*12*) reported that the hydrogen–deuterium equilibration reaction on the phthalonitrile–Na complex and the tetracyanopyrene–Na complex occurs mainly via the chemisorption mechanism, not the exchange mechanism. From the results of the latter work, it is difficult to understand that the hydrogen–deuterium exchange reaction on the anthracene–Na complex occurs via a monohydro compound. This confusion results from the fact that hydrogen–deuterium exchange reactions on aromatic–metal complexes are complicated by the existence of two possible reaction paths, in a manner similar to that in the exchange of oxygen isotopes between gaseous oxygen and solid oxide (*13*).

By making a preliminary experiment using the anthracene dianion, we found that a trace of water severely affects the reaction path of the catalyst and makes it a different species (*14*). Hence, in the experimental work, we were careful to remove all traces of water.

In the present work, the dependence of the catalytic activities on the sort of metal and also on the valency of aromatics in the triphenylene–alkali metal ion radical salt, prepared stoichiometrically, have been studied, and we briefly discuss the catalytic activities of the complexes. Throughout this study, careful attention has been given to the reaction time in order to obtain enough data to analyze the reaction mechanism, and the existence of the two paths is confirmed in these complexes. In addition, we discuss the relation between the hydrogen adsorption and the ortho–parahydrogen conversion; the discussed proposal is applicable to a catalyst on which an activated adsorption occurs.

Experimental Procedure

Commercially available triphenylene (Tp: Fig. 1 illustrates the structure) was recrystallized several times from its alcohol solution and then sublimed *in vacuo* in order to purify it. The triphenylene–alkali metal complexes, both mono- and dinegative ion salts, were stoichiometrically prepared as a precipitate from tetrahydrofuran (THF) solution. Since aromatic hydrocarbon anions are very reactive towards oxygen and moisture, the solvent (THF) had to be degassed carefully.

The formation of the triphenylene dinegative ion was detected by the color change in the THF solution from colorless to black. Figure 1 shows the optical absorption spectrum of the dinegative triphenylene ion in the THF solution. To obtain the solid salt, THF in the solution was evaporated completely to dryness.

In order to prepare the triphenylene mononegative ion, a known amount of alkali metal was reacted with the hydrocarbon. The formation of the mononegative ion was perceptible by the color change of the THF solution from colorless to blue. The absorption spectrum of the mononegative triphenylene ion is also shown in Fig. 1. These spectral responses agree with those reported by Hoijtink (*15*).

The rates and kinetics of the parahydrogen conversion, the hydrogen–deuterium exchange reaction, and the hydrogen–deuterium equilibration reaction were used to analyze the catalytic activities of the ion salts. All the experiments were carried out in this order.

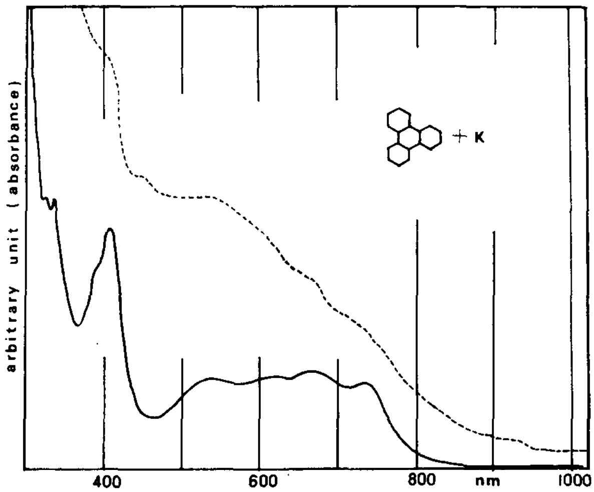

Fig. 1. The absorption spectra of mononegative and dinegative triphenylene ion in THF solution (potassium as a counterion): (—) mononegative ion; (- - -) dinegative ion.

Whenever the exchange reaction was carried out over a catalyst, the species were rejuvenated in advance with hydrogen gas several times in order to eliminate the exchanged and/or chemisorbed deuterium of the preceding reaction from the ion salt, and the hydrogen was evacuated for 4–5 hr.

The quantitative analysis of the hydrogen mixtures, p-H_2 + o-H_2 or H_2 + HD + D_2, was carried out by means of a gas-chromatographic method. The rate of adsorption of hydrogen was obtained by measuring the time course of the chromatographic area, which is proportional to the pressure of hydrogen.

RESULTS

As reported in a previous paper (*12*), the kinetics of a reaction on the aromatic–alkali metal ion salts take place by means of two processes; one is the "chemisorption process," and the other is the "exchange process." The "chemisorption process" is a reversible reaction of hydrogen–deuterium exchange in chemisorbed molecules on a catalytic surface, while the "exchange process" is an exchange reaction between gaseous deuterium and the hydrogen atom of the catalyst. In the present investigation, these kinetics were studied as a function of the sort of metal and of the valency of the aromatic anion.

I. Hydrogen–Deuterium Exchange Reaction

It was observed that there were characteristic patterns in the time course of the exchange reaction over the rejuvenated sample, as had been reported by Tsuda (*10*). Figure 2 shows a typical example of these patterns, obtained using the following equation;

$$k_D = \frac{2.3}{t} \log \frac{D_0}{D_t}, \qquad (1)$$

where D_0 and D_t represent the concentration of deuterium in the gas phase initially and after t hours, respectively, and where k_D is an apparent first-order rate constant. The exchange reaction over the rejuvenated catalyst does not follow the simple first-order law, judging from Fig. 2. In order to clarify this complexity, the difference in the progress of the reaction due to the different states of the same sample, fresh and rejuvenated, is illustrated in Fig. 3. The fresh sample, degassed for 5 hr immediately after having been synthesized, obeyed Eq. (1) simply, while the pattern was somewhat complicated in the rejuvenated one, as shown in Fig. 2. Though the kinetic behavior in the rejuvenated sample is complicated, we can assert from Fig. 3 that the reaction rate of Stage II (Fig. 3) equals that of the fresh one.

The hydrogen–deutrium equilibration re-

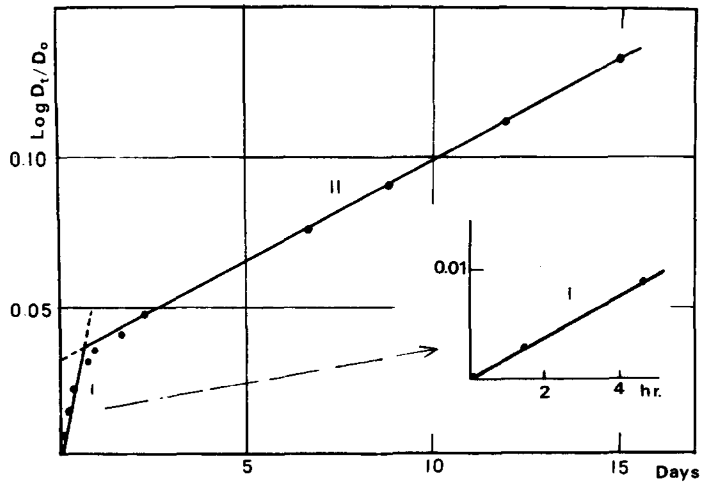

FIG. 2. The hydrogen–deuterium exchange reaction on the Tp–Rb(I) complex at 70°C. For the meaning of Stages I and II, see text.

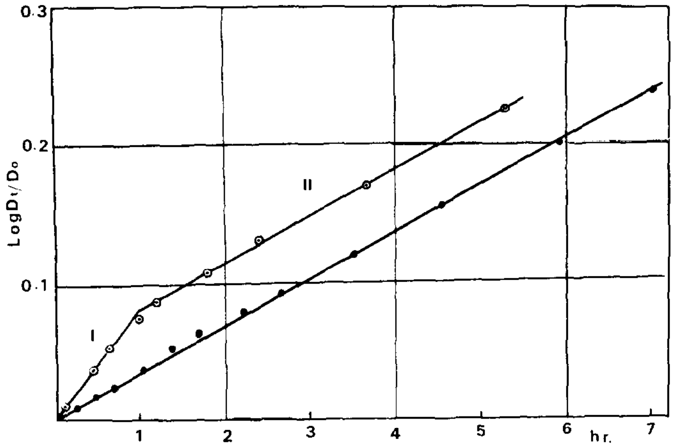

FIG. 3. The hydrogen-deuterium exchange reaction on the Tp-Rb(II) complex at 70°C: (●) fresh sample (⊙) rejuvenated sample. Both samples were degassed for 5 hr before reaction.

action, the rate constant of which is denoted by k_{eq}, was carried out on the Tp–Rb sample; the findings are listed in Table 1.

II. Ortho–Parahydrogen Conversion

The rate of approach to equilibrium, in agreement with the results of other experiments (*1*), followed a first-order law at a constant pressure at all temperature studied with the rate constant $k_{o \cdot p}$, where

$$k_{o \cdot p} = \frac{2.3}{t} \log \frac{C_0 - C_e}{C_t - C_e}, \tag{2}$$

and where the subscripts e, 0, and t refer to the concentrations of parahydrogen at equilibrium, time zero, and time t, respectively. The rate constants and the activation energies ($E_{o \cdot p}$) for six species of alkali metal ion salts are summarized in Table 2. It is evident, in the catalytic activity of the ion salts with the same metal cation, that the $k_{o \cdot p}$ of the divalent ion salt is 10^2 or 10^3 times larger than that of the monovalent salt. With regard to the divalent complexes, the tendency of the rate constant as a function of the sort of metal is Cs > K > Rb at 60°C, but Cs > Rb > K at 80°C, because of the enormously large activation energy ($E_{o \cdot p}$) for the Rb(II) complex. In the case of monovalent ion salts, the rate constant decreases also in the order of Cs, Rb, and K.

III. Simultaneous Measurement of Hydrogen Adsorption and Ortho–Parahydrogen Conversion

A typical example of the pressure decay of hydrogen caused by adsorbing on the samples, fresh and rejuvenated, is shown in Fig. 4 after calibration the pressure change by sampling. Figures 5 and 6 show the relation between the pressure decay of hydrogen and the hydrogen conversion. Further, the time course of the conversion over a fresh sample is shown in Fig. 7, together with the theoretical curve.

The various rate parameters obtained by analyzing the experimental results are col-

TABLE 1

THE RATE CONSTANT FOR H_2–D_2 EQUILIBRATION REACTION (70°C)

Ion salt	k_{eq} (hr^{-1})	$k_{o \cdot p}$ (hr^{-1})	k_c (hr^{-1})	k_e (hr^{-1})
Tp-Rb(I)[a]	2.8×10^{-2}	7.3×10^{-2}	4.4×10^{-2}	5.9×10^{-4}
Tp-Rb(II)[a]	1.6×10^{-1}	1.1×10^{0}	1.8×10^{-1}	2.7×10^{-3}

[a] Tp-Rb(I) stands for a monovalent ion and Tp-Rb(II) means a divalent ion of triphenylene having rubidium as a counter ion. These are different samples from those in Table 2.

TABLE 2
THE RATE CONSTANTS AND THE ACTIVATION ENERGIES FOR VARIOUS TRIPHENYLENE–ALKALI METAL ION SALTS

Ion salt	Temp (°C)	$k_{o.p}$ (hr^{-1})	k_c (hr^{-1})	k_e (hr^{-1})	$E_{o.p}$ (kcal/mole)[a]
Tp–K(I)	80	1.0×10^{-1}	2.2×10^{-2}	8.1×10^{-5}	7
Tp–K(II)	60	2.3×10^{0}	1.9×10^{-1}	3.9×10^{-3}	6
	−197	1.8×10^{-3}	—	—	
Tp–Rb(I)	80	—	6.2×10^{-2}	1.2×10^{-3}	8
	−197	4.1×10^{-3}	—	—	
Tp–Rb(II)	60	1.3×10^{0}	1.3×10^{-1}	5.6×10^{-4}	19
Tp–Cs(I)	80	2.2×10^{-1}	5.1×10^{-1}	1.0×10^{-3}	19
Tp–Cs(II)	60	9.9×10^{0}[b]	5.1×10^{-1}	1.7×10^{-2}	7
	−197	2.4×10^{-3}	—	—	

[a] Value at temperature range 0–80°C.
[b] At 30°C.

lected in Table 3. The notation in Table 3 is mentioned in the next section.

THEORETICAL TREATMENT

It has already been pointed out that there are two processes in the hydrogen–deuterium equilibration reaction over the aromatic–alkali metal ion radical salts (*10*, *12*). These processes were phenomenologically presented as two reaction stages, I and II, in Fig. 2; the "chemisorption process" is the rate-determining step in the region of Stage I, and the "exchange process" in Stage II.

I. Adsorption and Desorption Rate Constants

The remarkable difference in hydrogen adsorption between fresh and rejuvenated samples of triphenylene(Tp)–alkali metal complexes, as illustrated in Fig. 4, can be explained using the successive reaction model depicted in Fig. 8. The model is simplified in the following scheme;

$$P \underset{k_{-1}}{\overset{k_1}{\rightleftharpoons}} P_s \xrightarrow{k_2} \text{complex state,} \qquad (3)$$

where P and P_s are the pressures of gaseous hydrogen and of the absorbed hydrogen on

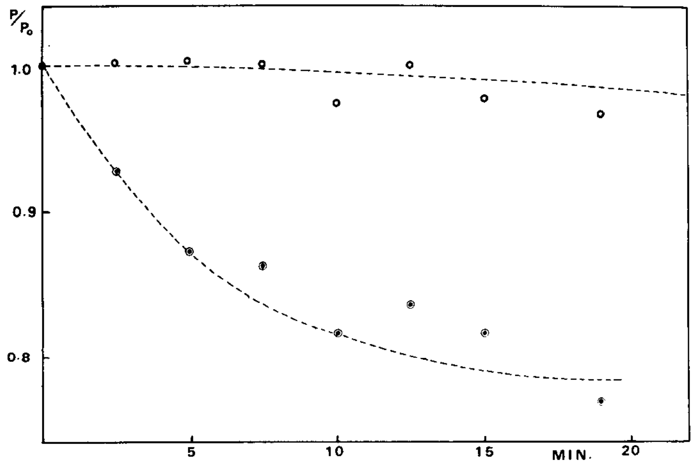

FIG. 4. Pressure decay of fresh sample (⊙) at 80°C and of rejuvenated sample (○) at 90°C for Tp–K(II) ion radical salt. Initial pressure is denoted by P_0. (- - -) Calculated curves from Eqs. (11) and (12).

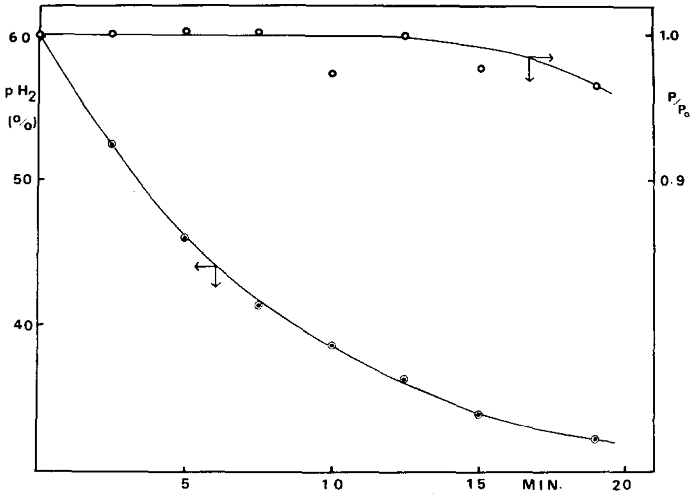

FIG. 5. The simultaneous measurement of an ortho–parahydrogen conversion and a hydrogen adsorption for Tp–K(II) rejuvenated sample at 90°C: (⊙) rate of conversion; (○) pressure of hydrogen.

the catalyst. Further, k_1 and k_{-1} are the rate constants of adsorption and desorption respectively, while k_2 is the rate constant of the hydrogen-addition reaction with the complexes. The following equations are obtained by using the notations in Eq. (3):

$$-\frac{dP}{d_s} = k_1P - k_{-1}P_s, \tag{4}$$

$$-\frac{dP_s}{d_s} = (k_{-1} + k_2)P_s - k_1P. \tag{5}$$

First, we will describe qualitatively the initial behavior of the reaction, represented in Eq. (3). For the fresh sample, we introduce $P_s = 0$ in Eq. (4), because no hydrogen adsorbs on the surface of the salt at the initiation of the reaction; then P is described as

$$P = P_0e^{-k_1t}. \tag{6}$$

Equation (6) expresses approximately the initial adsorption curve on the fresh sample and offers a means for deciding k_1.

When a surface is saturated with adsorbed hydrogen, gaseous hydrogen equilibrates with the adsorbed hydrogen; no additional adsorption occurs except with the adsorbed hydrogen is diminished by a re-

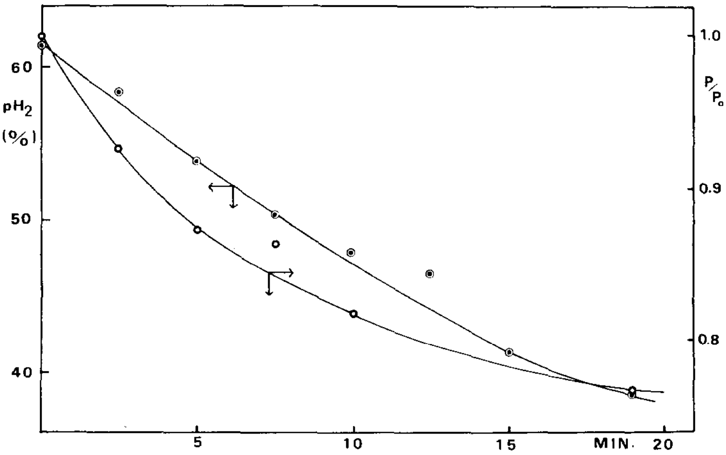

FIG. 6. The simultaneous measurement of an ortho–parahydrogen conversion and a hydrogen adsorption for Tp–K(II) fresh sample at 80°C: (⊙) rate of conversion; (○) pressure of hydrogen.

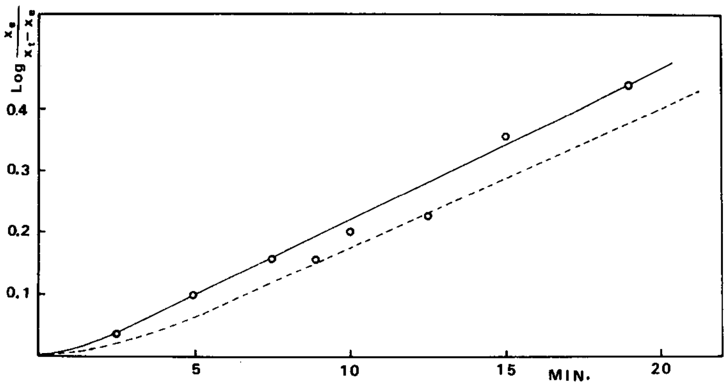

FIG. 7. The time course of ortho–parahydrogen conversion when hydrogen is adsorbing on the Tp–K(II) fresh sample at 80°C: (- - -) calculated curve predicted by Eq. (18); and (—) experimental data.

action with substrates; that is to say, P_s equilibrates to P. Therefore, we obtain $-(dP/dt) = 0$ as the initial adsorption rate, and Eqs. (4) and (5) are:

$$P = P_0, \tag{7}$$

$$P_s = KP, \tag{8}$$

where $K = k_1/k_{-1}$ is the adsorption–desorption equilibrium constant.

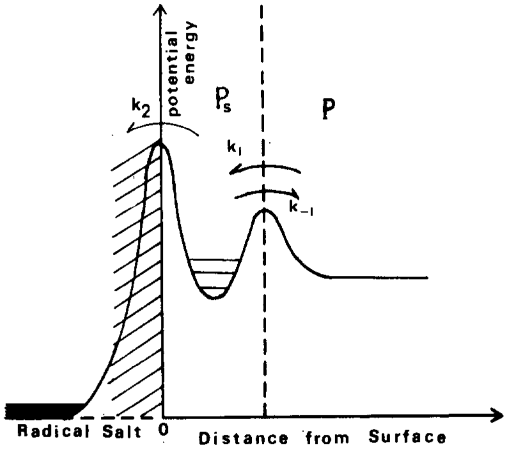

FIG. 8. The schematic representation of hydrogen adsorption on the ion radical salt surface. The right side of the broken line indicates a free gas phase and its left side is a surface adsorbed phase such as a chemisorbed state. P is the gaseous hydrogen pressure in the free space, while P_s is the surface pressure of hydrogen equivalent to the concentration of adsorbed hydrogen. k_1, k_{-1}, and k_2 stand for the rate constants of adsorption, desorption and the reaction between adsorbed hydrogen and substrate. The interior of the radical salt is displayed by shadowed lines.

The exact analytical solution of Eqs. (4) and (5), very complicated in form, can be simplified if it is taken into account that $k_1, k_{-1} \gg k_2$;

$$P_s = c_1 e^{s_1 t} + c_2 e^{s_2 t}, \tag{9}$$

$$P = \left[P_0 - k_{-1} \left\{ \frac{c_1}{s_1 + k_1} \left(1 - e^{(s_1 + k_1) t}\right) + \frac{c_2}{s_2 + k_1} \left(1 - e^{(s_2 + k_1) t}\right) \right\} \right] e^{-k_1 t}, \tag{10}$$

where $s_1 = -k_2/2$, $s_2 = -k - k_2/2$, and $k = k_1 + k_{-1}$. Further, c_1 and c_2 are the integral constants, which are determined by the initial conditions.

We can apply this treatment to typical initial conditions. In a system having a surface saturated with adsorbed hydrogen, we obtain

$$\frac{P}{P_0} = \frac{k_2}{2k}\left(K - \frac{1}{K}\right) e^{-k_1 t} + \left(1 + \frac{k_2}{2kK}\right) e^{-(k_2/2)t} - K \frac{k_2}{2k} \exp\left[-\left(k + \frac{k_2}{2}\right) t\right] \tag{11}$$

from Eq. (10). For a clean surface, the following equation is obtained;

$$\frac{P}{P_0} = \frac{k_{-1}}{k} e^{-(k_2/2)t} \left[\left(1 + \frac{k_2}{2k_1}\right) + K\left(1 - \frac{k_2}{2k_{-1}}\right) e^{-kt} \right]. \tag{12}$$

From Eqs. (12) and (6), the rate constants, k_1, k_{-1}, and k_2, are obtained by means of

TABLE 3
THE VALUES OF THE RATE CONSTANTS (hr^{-1}) FOR HYDROGEN CONVERSION

Sample	$k_{o.p}$ Fresh	$k_{o.p}$ Rejuvenated	k_1	k_{-1}	k_2	α
Tp-K(II)	3.3×10^0	4.3×10^0	2.9×10^0	1.0×10^1	1.9×10^{-1}	1.5
Tp-Rb(II)	—	5.0×10^0	1.8×10^0	4.5×10^0	2.7×10^{-3}	2.7

the curve-fitting method; they are listed in Table 3.

The broken lines in Fig. 4 are the curves calculated using Eqs. (11) and (12) with the rate parameters thus obtained.

The time course of P_s, which is equivalent to the variation in the surface coverage with the time, is also derived from Eq. (9);

$$\frac{P_s}{P_0} = \frac{k_1}{k} e^{-(k_2/2)t} (1 - e^{-kt}). \qquad (13)$$

In Fig. 9, the surface saturation curve [Eq. (13)] for the fresh Tp-K(II) sample is plotted against the time.

II. The Rate Constant for Ortho-Parahydrogen Conversion

We derive the conversion rate constant, $k_{o\text{-}p}$, from the adsorption and desorption parameters by means of a hypothesis concerning the adsorbed layers; the ideal gas model for hydrogen gas and its adsorbed phase is introduced. For the chemisorption process, the model is illustrated in Fig. 8.

From the above assumption, the progression of the ortho-parahydrogen conversion is given as:

$$-\frac{dx_t}{dt} = k_{-1}\frac{P_s}{P}(x_t - x_e), \qquad (14)$$

where x_t and x_e stand for parahydrogen content at time t and at equilibrium, respectively.

On the other hand, the experimental rate equation is given by

$$-\frac{dx_t}{d_t} = k_{o\text{-}p}(x_t - x_e). \qquad (15)$$

From Eqs. (14) and (15) it follows that

$$k_{o\text{-}p} = k_{-1}\frac{P_s}{P}. \qquad (16)$$

Because P_s and P are functions of time, $k_{o\text{-}p}$ depends on the time and is not a rate constant in the strict sense. However, $k_{o\text{-}p}$ is apparently constant at the beginning of conversion over a rejuvenated sample from Eq. (8), while P_s changes drastically over a fresh sample in the initial reaction period, thus causing a notable change in $k_{o\text{-}p}$.

Under these conditions of adsorption-de-

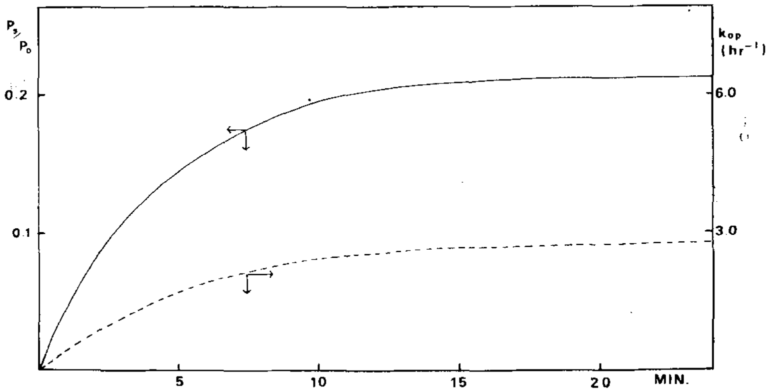

FIG. 9. Calculated curves for the surface saturation and the ortho-parahydrogen conversion rate constant for the fresh Tp-K(II) sample: (—) surface saturation curve with Eq. (13); (- - -) ortho-parahydrogen conversion rate constant with Eq. (18).

sorption equilibration, $k_{o\cdot p}$ is given, by substituting Eq. (8) into Eq. (16), as:

$$k_{o\cdot p} = k_1. \tag{17}$$

Thus, the rate constant of ortho–parahydrogen conversion equals the adsorption rate constant, and this is the maximum value of $k_{o\cdot p}$.

For the fresh samples, after directly substituting the representation of P_s and P into Eq. (16), we obtain;

$$k_{o\cdot p} = k_1 \frac{1 - e^{-kt}}{[1 + (k_2/2k_1)] + K[1 - (k_2/2k_{-1})]\, e^{-kt}} \tag{18}$$

Figure 9 shows the curve calculated for $k_{o\cdot p}$ of the fresh Tp–K(II) sample using Eq. (18).

In the above treatment, we assumed that the adsorbed particles move freely over a catalyst surface. If the free motion of particles on the surface is restricted, the free surface space is reduced. When the contribution of this factor is introduced, Eq. (16) is rewritten as

$$k_{o\cdot p} = \alpha k_{-1} \frac{P_s}{P}, \tag{19}$$

where α is a measure of the mobility of a particle; the more α deviates from unity, the more the adsorbed particles are immobile.

DISCUSSION

In the experimental work, it was found that the hydrogen–deuterium exchange reaction does not obey the simple first-order law when the *rejuvenated* aromatic–alkali metal complexes are used as the catalysts. This irregular phenomenon, shown in Fig. 2, is caused by the fact that the complex catalyst itself reacts with the gaseous hydrogen. The system investigated here is closely analogous to the isotope exchange of oxygen on a solid metal oxide. It has been reported that there are two exchange paths; one of them is the reaction between gaseous oxygen and a solid oxide, while the other is that among gaseous oxygen species adsorbed on the oxide.

Consequently, in this hydrogen exchange system, the following two possible reaction paths should be considered; (1) the reaction between gaseous hydrogen and the ion-salt catalyst (exchange process) and (2) the reaction among gaseous hydrogen adsorbed on the catalyst (chemisorption process).

Because no adsorbed hydrogen exists on the *fresh* sample, we can suppose the hydrogen–deuterium exchange reaction conducted over the fresh sample via Mechanism (1). However, in the case of the hydrogen–deuterium exchange reaction over the rejuvenated sample, as in the hydrogen–deuterium equilibration reaction, these two competitive reaction paths, (1) and (2), are possible on account of adsorbed hydrogen. As described in the preceding section, it was found on the rejuvenated sample that the precursory reaction (Stage I of Fig. 3) is faster than the latter one (Stage II), whose rate constant coincided with that of the fresh sample. This behavior can be explained by saying that deuterium gas reacts with adsorbed hydrogen at the first stage, and that then the gaseous deuterium reacts with the bulk hydrogen.

Hereafter, we will denote k_c as the rate constant of Stage I and k_e as that of Stage II in Fig. 2.* Consequently, k_e coincides with the rate constant of the deuterized reaction of the catalyst. The rate constants of the hydrogen–deuterium equilibration (k_{eq}) and the ortho–parahydrogen conversion ($k_{o\cdot p}$), and also both k_c and k_e obtained from the hydrogen–deuterium exchange reaction are listed in Table 1. From Table 1, the rate constants can be said to have the following tendency: $k_{o\cdot p} > k_c \simeq k_{eq} \gg k_e$. Hence, we can conclude that the hydrogen–deuterium equilibration reaction and the ortho–parahydrogen conversion occur via the chemisorption process, not via the exchange process. The divalent ion salts have stronger catalytic activities than the monovalent ion salts with the same metal cations

---

* The separation of these two rate constants, k_c and k_e, had been made graphically, and each constant calculated as a tangent of the degree of reaction vs the time *(10)*. In this investigation, however, we determined them by means of the least-squares method, using the initial k_c and k_e values obtained graphically as in Ref. *(10)*. The measure of dispersion was about 10^{-4} in all cases.

by one order of magnitude for the chemisorption process, while they show the same trend in the exchange process; these findings are in accordance with those of a previous paper (*3*). It may also be mentioned that the chemisorption process is the main path for the hydrogen–deuterium exchange reaction over the rejuvenated sample in both monovalent and divalent salts, considering the fact that k_c is much larger than k_e.

As for the catalytic activities, there is a tendency for k_c and, accordingly, $k_{o\text{-}p}$ to decrease monotonically with Cs, Rb, and K for the monovalent ion salts, but there is some complexity in the case of the divalent ion because of the large activation energy of Rb salt. On the other hand, there is no simple relation with respect to k_e. A report on the hydrogen–deuterium exchange reaction over aromatic–alkali metal complexes has stated that the reaction occurred via aromatics as intermediates (*16*). This treatment so simplifies the catalytic system that it neglects the fact that the two reaction paths have different metal dependencies. The alkali metal will certainly play a different role in the two reaction paths. The simple relation between the kind of metal and the $k_{o\text{-}p}$ value indicates that the metal plays an important role in the conversion.

The pressure decay of hydrogen over the catalysts, as illustrated in Fig. 4, can be expressed successfully by theoretical curves. The good agreement of k_1 with $k_{o\text{-}p}$ over the rejuvenated sample, as predicted by the theory, is proved by Table 3. Moreover, we can expect from Eq. (18) that $k_{o\text{-}p}$ measured over the fresh sample will be smaller than the value measured over the rejuvenated sample. This fact is also confirmed by Table 3. When we compare Fig. 9 with Fig. 7 in which the experimental rate constant $k_{o\text{-}p}$ of Eq. (15) is plotted against the time for the Tp–K(II) sample, we find a coincidence with the initial transient behavior. The theoretical curve in Fig. 7, calculated from Eq. (18), expresses the qualitative behavior of ortho–parahydrogen conversion, excluding the final slope. If the difference in the rate constant between the experimental value, 3.3, and the calculated value, 2.9, is taken into account, the theoretical curve approaches more closely the solid line of Fig. 7. A coincidence also appears in the time course of P_s with $k_{o\text{-}p}$, as shown in Fig. 9.

When a two-dimensional gas model is used for the surface state of adsorbed particles, one has to estimate the values of surface area, the number of sites and also the coverage (*17*). Hence, the formulation for the surface state reported in this paper is advantageous in its simplicity, because the estimation of the values mentioned above is not needed. This formulation can be expanded to a system in which the substrate does not react with adsorbed molecules, i.e., $k_2 = 0$, and makes an activated adsorption.

It is very interesting to compare this metal–organic system with an enzyme such as hydrogenase, which is a biological catalyst for the hydrogen–deuterium exchange reaction and also for the ortho–parahydrogen conversion (*18*, *19*). This enzyme contains iron atoms as a ferredoxin skeleton; the atoms are considered to be active sites. In view of the analogous constitutents (organics and metals), and also from the similarity in their activities, the mechanisms may be said to have something in common.

REFERENCES

1. Kondow, T., Inokuchi, H., and Wakayama, N., *J. Chem. Phys.* **43**, 3766 (1965).

2. Inokuchi, H., Wakayama, N., Kondow, T., and Mori, Y., *J. Chem. Phys.* **46**, 837 (1967).

3. Inokuchi, H., Mori, Y., and Wakayama, N., *J. Catal.* **8**, 288 (1967).

4. Wakayama, N., and Inokuchi, H., *J. Catal.* **11**, 143 (1968).

5. Ichikawa, M., Soma, M., Onishi, T., and Tamaru, K., *J. Phys. Chem.* **70**, 2069 (1966).

6. Ichikawa, M., Soma, M., Onishi, T., and Tamaru, K., *J. Catal.* **6**, 336 (1966).

7. Ichikawa, M., Soma, M., Onishi, T., and Tamaru, K., *Trans. Faraday Soc.* **63**, 997 (1967).

8. Ichikawa, M., Soma, M., Onishi, T., and Tamaru, K., *Trans. Faraday Soc.* **63**, 2529 (1967).

9. Ichikawa, M., Soma, M., Onishi, T., and Tamaru, K., *Bull. Chem. Soc. Jap.* **41**, 1739 (1968).

10. Tsuda, M., *Bull. Chem. Soc. Jap.* **43**, 3415 (1970).

11. Tanaka, S., Naito, S., Ichikawa, M., Soma, M., Onishi, T., and Tamaru, K., *Trans. Faraday Soc.* **66**, 976 (1970).

12. Wakayama, N., and Inokuchi, H., *J. Catal.* **11**, 143 (1968).

13. Klier, K., Nováková, J., and Jírů, P., *J. Catal.* **2**, 479 (1963).

14. Velthorst, N. H., and Hoijtink, G. J., *J. Amer. Chem. Soc.* **87**, 4529 (1965).

15. Hoijtink, G. J., *Mol. Phys.* **2**, 85 (1959).

16. Ichikawa, M., Soma, M., Onishi, T., and Tamaru, K., *Bull. Chem. Soc. Jap.* **43**, 3672 (1970).

17. Hayward, D. O., and Trapnell, B. M. W., "Chemisorption," p. 164. Butterworths, London, 1964.

18. Krasna, A. I., and Rittenberg, D., *J. Amer. Chem. Soc.* **76**, 3015 (1954).

19. Yagi, T., Tsuda, M., Mori, Y., and Inokuchi, H., *J. Amer. Chem. Soc.* **91**, 2801 (1969).